LOW LEVEL WARM AIR ADVECTION, JUNE 8-9, 1953

GEORGE C. HOLZWORTH AND CHARLES F. THOMAS

WBAN Analysis Center, U. S. Weather Bureau, Washington, D. C.

INTRODUCTION

Meteorologists have long realized the importance of warm air advection in the lower levels of the atmosphere—especially in relation to regions of active weather such as cloudiness and precipitation [1, 2]. Intimately tied to these regions of warm air advection and weather are fields of vertical motion and areas of surface pressure change. The effect of warm air advection in an air column contributing to a surface pressure fall and cold air advection contributing to a pressure rise is well understood [3]. However, in some discussions of temperate zone weather, warm and cold air advection are treated with reference to the usually observed attendant advection of high, cold and low, warm tropopauses, respectively. For instance, when it is pointed out that indicated warm air advection in the lower levels (500 mb. or lower) will likely lead to a buildup of higher surface pressures, what is really implied is that the lower warming will be more than balanced by the advection aloft of a high, cold tropopause. The upper level cold air advection is expected to more than compensate the lower warm air advection—there will be a density increase—and surface pressures will rise. Cooling in an air column contributes to a surface pressure rise and warming contributes to a fall. In all discussions the terminology should be consistent with the actual processes as well as with what is finally observed as the net result.

Since thickness lines are also isotherms of mean virtual temperature for the layer, the regions of warm air advection are those where the flow is against the thickness lines and directed from higher toward lower values. The spacing of the thickness lines depends on the magnitude of the thermal wind, which simply is the wind shear between the bottom and the top of the layer; the stronger the shear, the greater the gradient. At the same latitude geostrophic flow on a constant pressure surface depends on the contour spacing; the closer the spacing, the stronger the flow. Therefore, the indicated advection is inversely proportional to the quadrangular areas bounded by thickness lines and contours of a constant pressure surface through the thickness layer.

From a study of low level warm air advection during the period June 8–9, 1953, this paper presents some thickness and pressure change relationships, and, employing the displacement of thickness lines, some simple computations of vertical motion are made. The paper attempts to describe a clear and consistent picture of the general density changes occurring below 500 mb. and to reason the changes that must be taking place above 500 mb. to be mutually consistent with observed sea level pressure changes.

THICKNESS AND PRESSURE CHANGE RELATIONSHIPS

Figure 1 is a composite chart of the 1000-mb. contours and the 1000-500-mb. thickness lines for 0300 GMT on June 8, 1953. At this time the area of strongest warm air advection is indicated near the center of the chart by the concentration of the small quadrangular areas bounded by contours and thickness lines. Figure 2 is a composite 12-hour change chart, showing the 1000-mb. height change and the 1000-500-mb. thickness change from 1500 GMT, June 7 to 0300 GMT, June 8. Since thickness lines may be considered as fairly conservative, their movement can be attributed mainly to advection [4]. In figure 2 the area of positive thickness change shows where warming has actually occurred. A change of about 66½ feet in the 1000-500-mb. layer is equal to a mean virtual temperature change of 1° C.

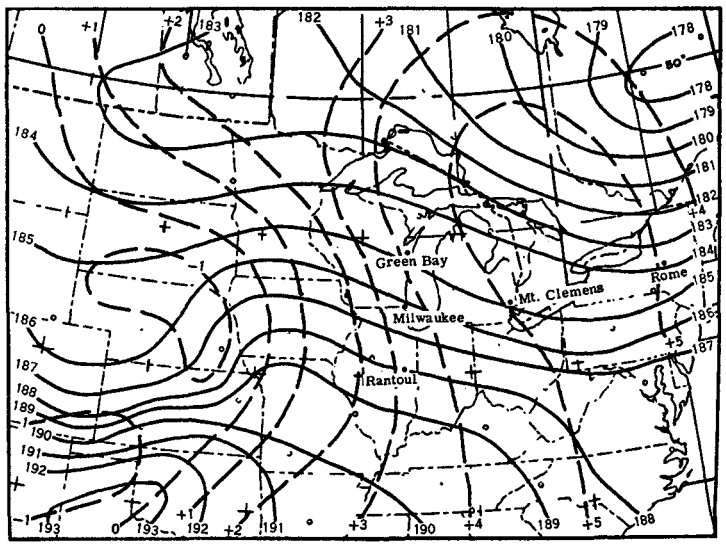

FIGURE 1.—Composite chart of 1000-500-mb thickness (solid lines) and 1000-mb. height (dashed lines) for 0300 GMT, June 8, 1953. Values are in hundreds of feet.

The actual contribution to the surface pressure fall by warming in the layer may be closely approximated from elementary considerations. If the 500-mb. height does not change and the 1000-mb. height falls, the 1000-500-mb. layer gets thicker (less dense) and contributes to a surface pressure fall. In this case the contribution to the surface pressure fall comes entirely from below 500 mb. However, if the 500-mb. height also falls, but not as much as the 1000-mb. height fall, then the contribution *of this layer* to the surface pressure fall is reduced. Since thickness changes are transmitted downward as pressure changes it is possible to compute the contribution of the particular layer to the surface pressure change. For instance, at Duluth, Minn. at 0300 GMT, June 8 (fig. 2) the 1000-500-mb. thickness has increased 200 feet, the 1000-mb. height has decreased 250 feet, and so the 500-mb. height has decreased 50 feet. Near sea level, pressure decreases with height at the rate of about 1 mb. per 28 feet, U. S. Standard Atmosphere. Since the 1000-mb. height fell 250 feet, the surface pressure fell about 9 mb. but since the 1000-500-mb. layer thickened only 200 feet, the contribution of this layer to the surface pressure fall is 4/5 or 80 percent. The remaining 20 percent must have come from above 500 mb. A slight contribution may come from below 1000 mb. but for practical purposes this is negligible.

Along the eastern edge of the surface Low center (fig. 1) only slight warming is occurring in the 1000-500-mb. layer (fig. 2). But in this same zone rather pronounced 1000-mb. height falls are taking place. As a matter of fact, just a little farther east is located the center of 1000-mb. height fall, enclosed within a −300-foot isallohypse, and through this center runs the relative isallohypse of 100-foot increase in thickness of the 1000-500-mb. layer. Thus, in this area the decrease in density of the 1000-500-mb. layer accounts for only about one-third of the observed sea level pressure fall. Consequently the main contribution of density decrease to sea level pressure fall must come from above the 500-mb. level.

Eastward of the main center of 1000-500-mb. thickness increase (fig. 2) is the area where warming (increased thickness) exactly balances the observed sea level pressure fall; here is also the zone where the 500-mb. height change is zero. This does not mean that density changes are not taking place above 500 mb., undoubtedly they are, but they are counterbalancing each other so that the net effect at 500 mb. and below is zero.

Farther eastward toward the High center, but in the region of positive 1000-500-mb. thickness change and negative 1000-mb. height change, low level warming accounts for a greater pressure fall than is actually observed; density increase above 500 mb. must be occurring to compensate the excess density decrease below. Near the western edge of the High center this effect is even

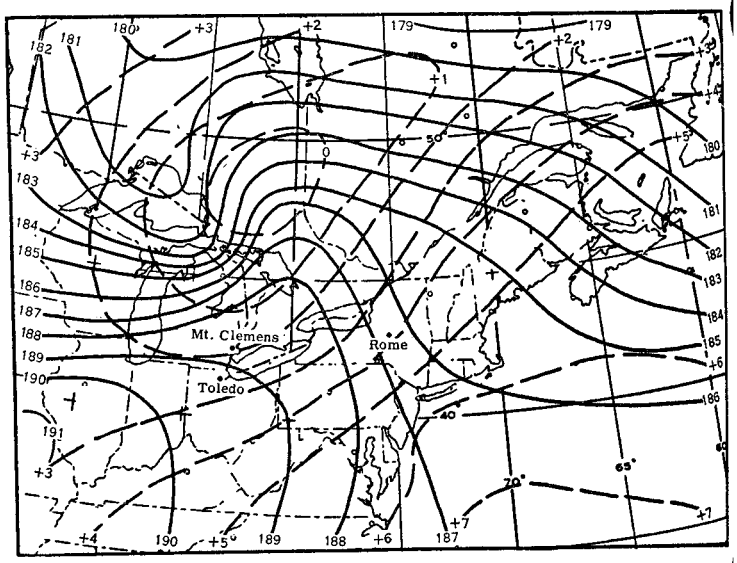

FIGURE 3. Composite chart of 1000-500-mb. thickness and 1000-mb. height for 1500 GMT, June 8, 1953.

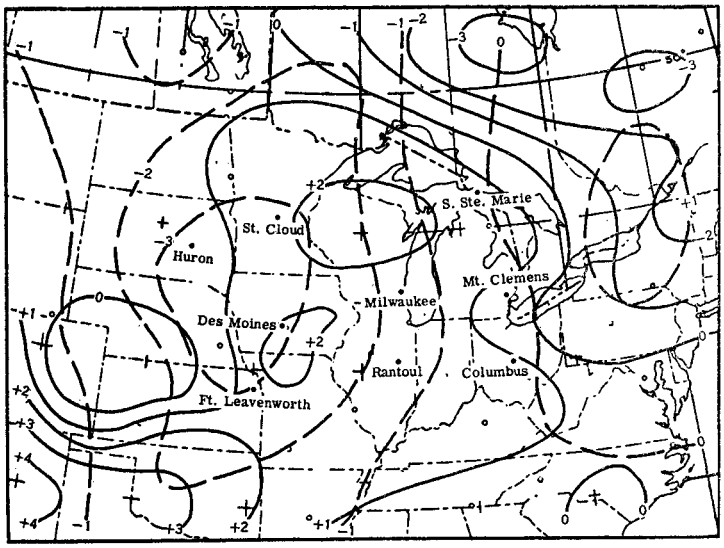

FIGURE 2.—Composite chart of 12-hour change of the 1000-500-mb. thickness (solid lines) and 1000-mb. height (dashed lines) from 1500 GMT, June 7 to 0300 GMT, June 8. Values are in hundreds of feet.

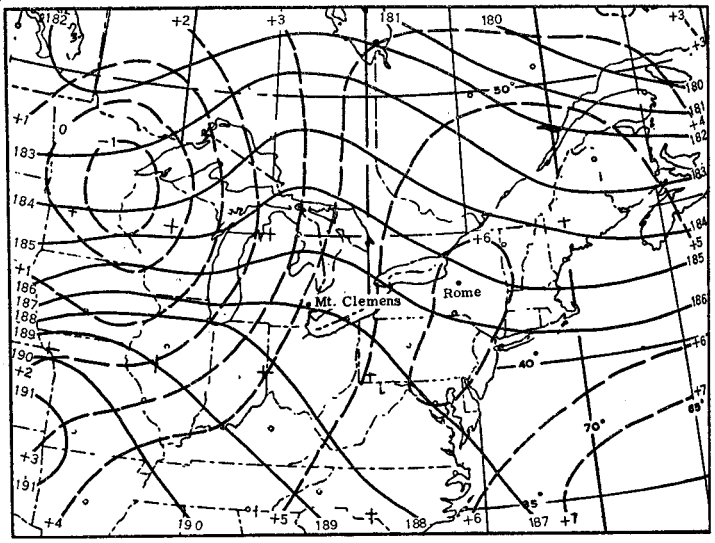

FIGURE 4.—Composite chart of 1000-500-mb. thickness and 1000-mb. height for 0300 GMT, June 9, 1953.

better illustrated. For here the sea level pressure is rising in spite of warming in the 1000-500-mb. layer.

Through the High center the thickness change is small and negative, and contributes slightly to the observed rise in surface pressure. Along the eastern edge of the High center the increase in density of the 1000-500-mb. layer becomes the main source of rising sea level pressure, and is balanced by a density decrease above 500 mb.

Thus, in this case one is led to the following picture of the balance of density decrease and increase above and below 500 mb. in contributing to sea level pressure change: Along the eastern edge of the Low center warming occurs below 500 mb., but the main contribution of density decrease to sea level pressure fall comes from above 500 mb. About half way from Low to High, low level warming completely accounts for the observed sea level pressure fall; the net effect from above 500 mb. is zero. A little farther east, low level warming accounts for more pressure fall than is observed so increased density above 500 mb. occurs. Near the High center low level cooling becomes most effective and therefore the amount of density increase at upper levels diminishes.

Figures 3 and 4 show how the areas of indicated warm air advection moved from southwest to northeast, and figures 5 and 6 show the 12-hour changes of 1000-500-mb.

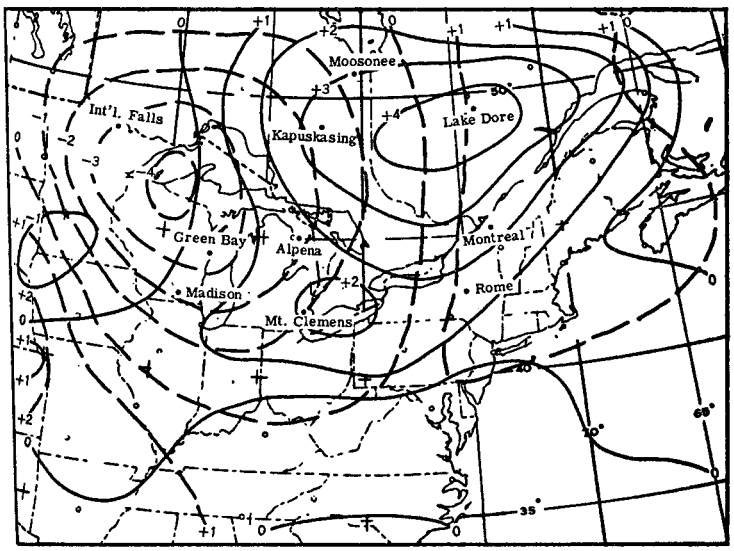

FIGURE 5.—Composite chart of 12-hour change of 1000-500-mb. thickness and 1000-mb. height from 0300 GMT to 1500 GMT, June 8, 1953.

TABLE 1.—*Relationship of 1000-500-mb. thickness change to surface pressure and 500-mb. height changes*

1500 GMT, June 7, to 0300 GMT, June 8, 1953

Station	ΔH_{1000}	$\Delta Z_{1000-500}$	ΔH_{500}	Δp
	Feet	*Feet*	*Feet*	*Millibars*
Huron, S. Dak	−320	+70	−250	−11.5
St. Cloud, Minn	−335	+175	−160	−12
Sault Ste. Marie, Mich	−20	+160	+140	−1
Des Moines, Iowa	−305	+210	−95	−11
Milwaukee, Wis	−150	+160	+10	−5
Mount Clemens, Mich	−25	+55	+30	−1
Fort Leavenworth, Kans	−285	+145	−140	−10
Rantoul, Ill	−140	+180	+40	−5
Columbus, Ohio	−20	+105	+95	−1
0300 GMT, June 8 to 1500 GMT, June 8, 1953				
Moosonee, Ontario	−60	+300	+240	−2
International Falls, Minn	−320	−80	−400	−11.5
Kapuskasing, Ontario	−165	+320	+155	−6
Lake Dore, Quebec	+105	+425	+530	+4
Green Bay, Wis	−310	+50	−260	−11
Alpena, Mich	−210	+165	−45	−7.5
Montreal, Quebec	+110	+235	+345	+4
Madison, Wis	−225	+25	−200	−8
Mount Clemens, Mich	−100	+205	+105	−3.5
Rome, N. Y	+105	+145	+250	−4
1500 GMT, June 8 to 0300 GMT, June 9, 1953				
Moosonee, Ontario	−350	−40	−390	−12.5
Alpena, Mich	−265	+40	−225	−9.5
Montreal, Quebec	−230	+155	−75	−8
Caribou, Maine	−60	+120	+60	−2
Milwaukee, Wis	+50	+100	+150	+2
Mount Clemens, Mich	−210	+150	−60	−7
Buffalo, N. Y	−250	+210	−40	−9
Rome, N. Y	−225	+135	−90	−8
Portland, Maine	−20	+85	+65	−1.5

ΔH_{1000}=12-hr. change in height of 1000-mb. level
ΔH_{500}=12-hr. change in height of 500-mb. level
$\Delta Z_{1000-500}$=12-hr. change in 1000 to 500-mb. thickness
Δp=12-hr. change in sea level pressure

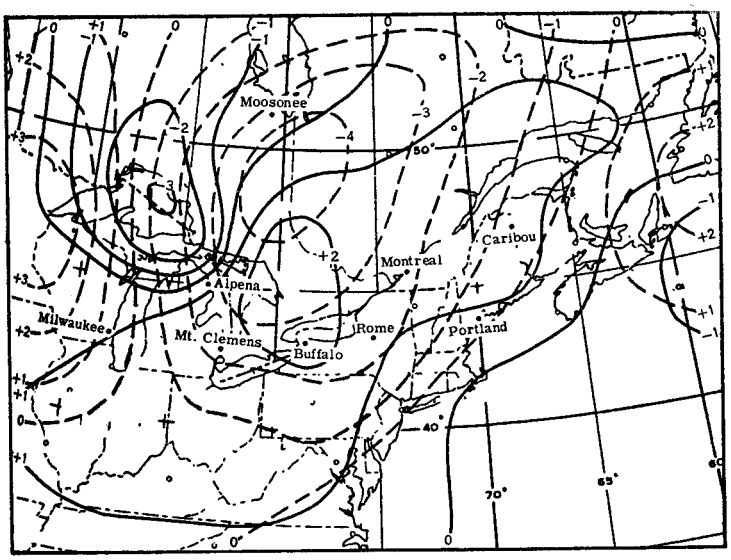

FIGURE 6.—Composite chart of 12-hour change of 1000-500-mb. thickness and 1000-mb. height from 1500 GMT, June 8 to 0300 GMT, June 9, 1953.

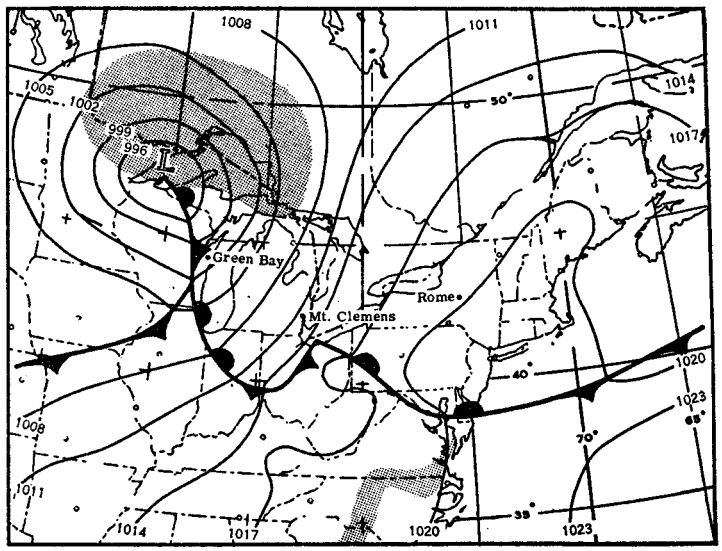

FIGURE 7.—Sea level weather chart for 1830 GMT, June 8, 1953. Shading represents the area where precipitation is occurring.

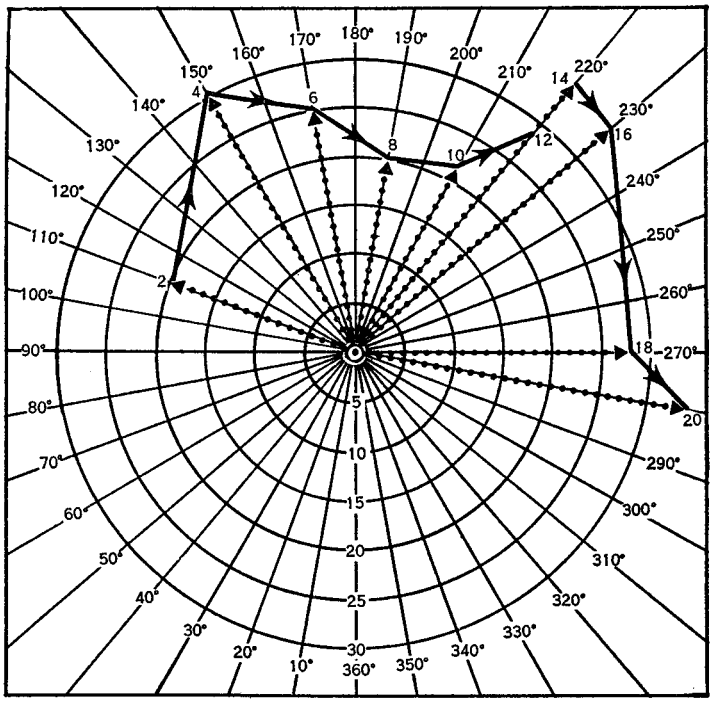

FIGURE 8.—Hodograph for Milwaukee, Wis., at 0300 GMT, June 8, 1953. The dotted vector is the observed wind in knots. The numbers on the periphery indicate the direction from which the wind is blowing. The figure near the vector head is the elevation in thousands of feet. The heavy vectors, indicating warm advection, are the thermal or shear vectors. For clarity the direction of the shear is shown along only some of the thermal vectors.

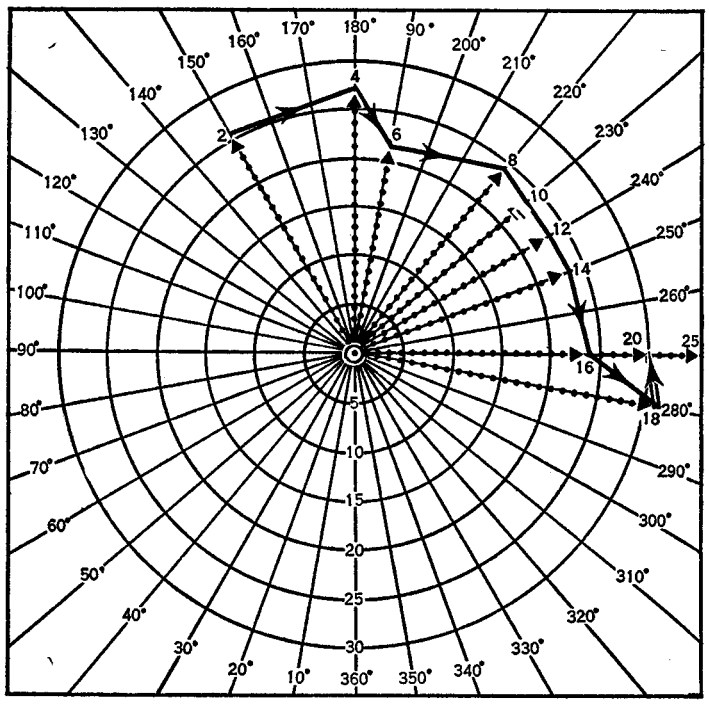

FIGURE 10.—Hodograph for Rantoul, Ill., at 0300 GMT, June 8, 1953.

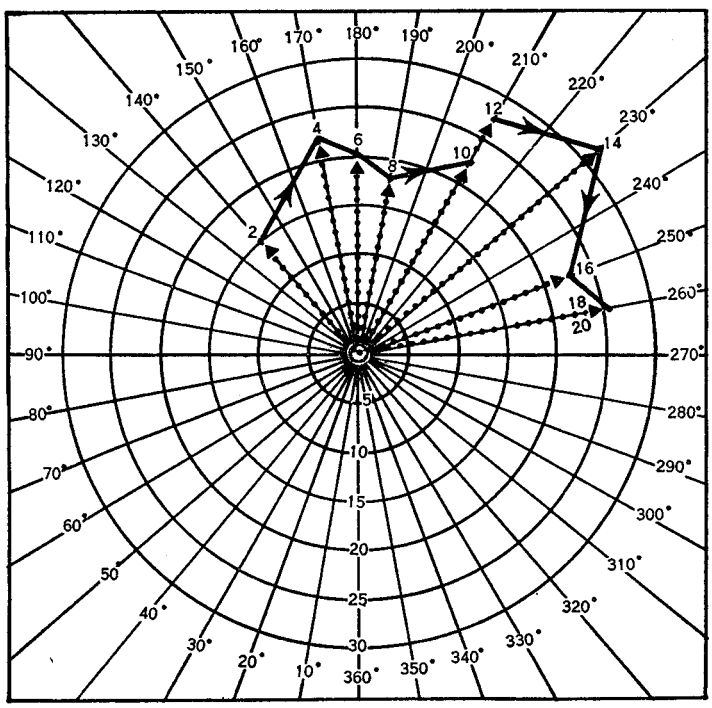

FIGURE 9.—Hodograph for Green Bay, Wis., at 0300 GMT, June 8, 1953.

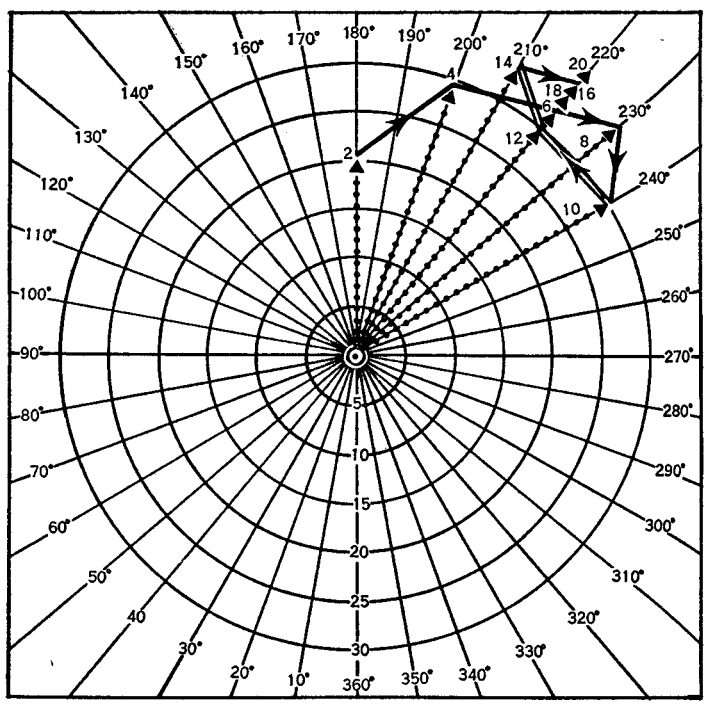

FIGURE 11.—Hodograph for Mount Clemens, Mich., at 1500 GMT, June 8, 1953.

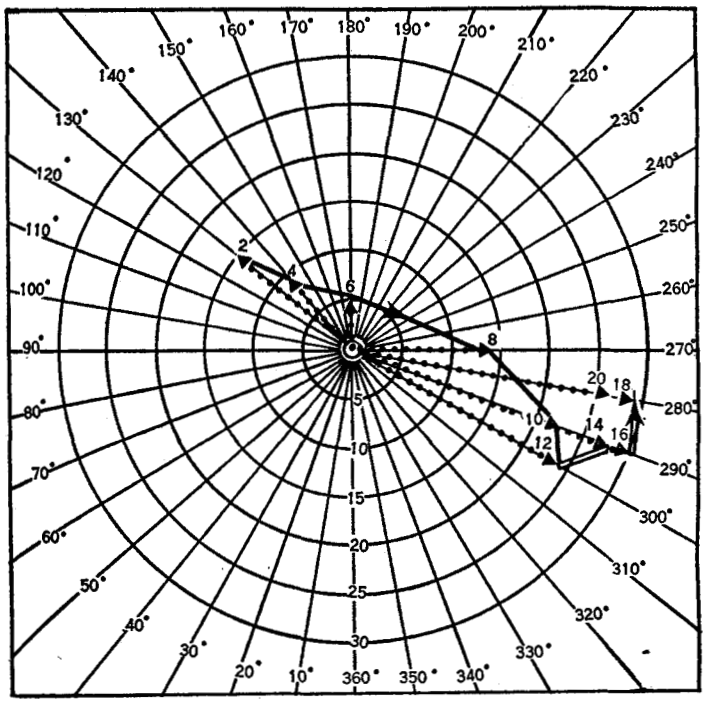

FIGURE 12.—Hodograph for Rome, N. Y., at 1500 GMT, June 8, 1953.

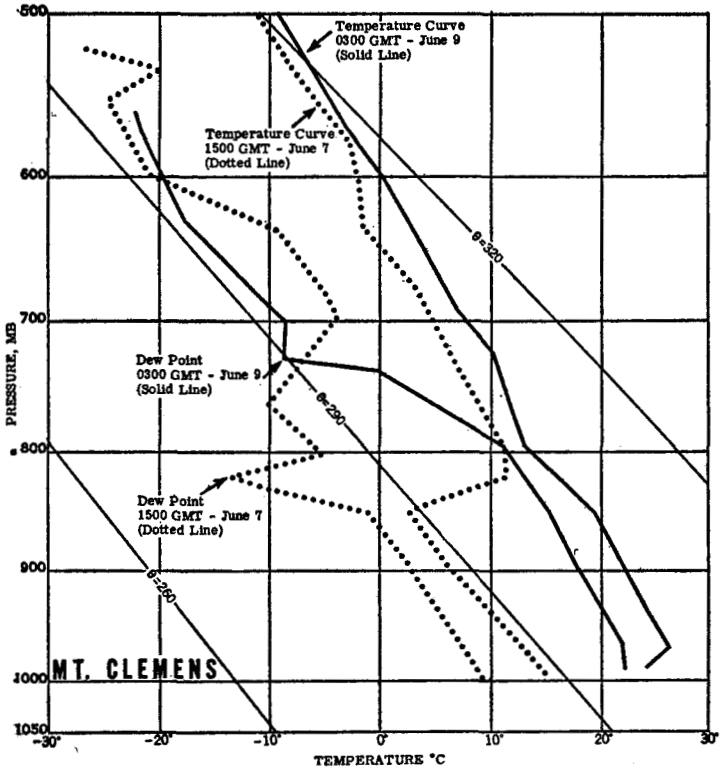

FIGURE 14.—Upper air soundings over Mount Clemens, Mich., at 1500 GMT, June 7 and 0300 GMT, June 9, 1953.

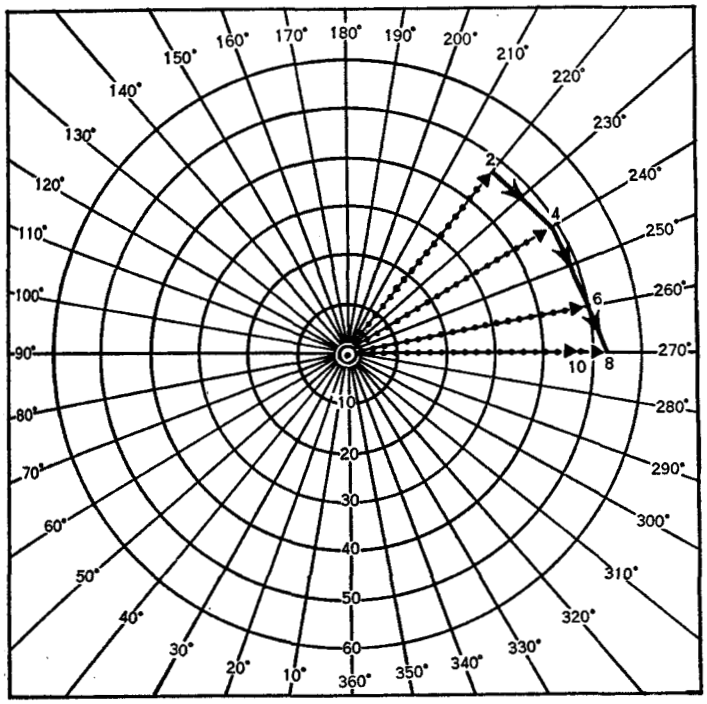

FIGURE 13.—Hodograph for Toledo, Ohio, at 0300 GMT, June 9, 1953.

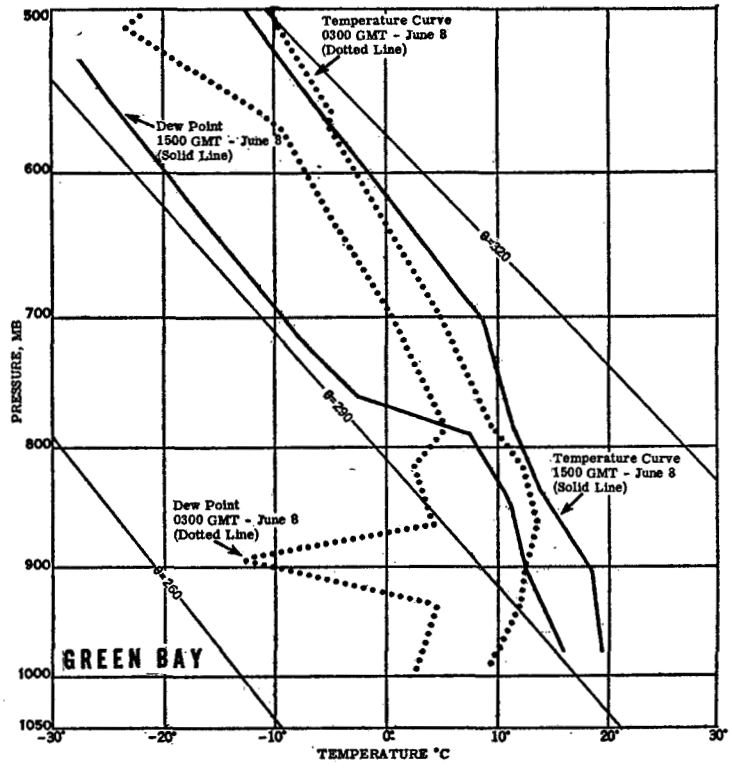

FIGURE 15.—Upper air soundings over Green Bay, Wis., at 0300 GMT and 1500 GMT, June 8, 1953.

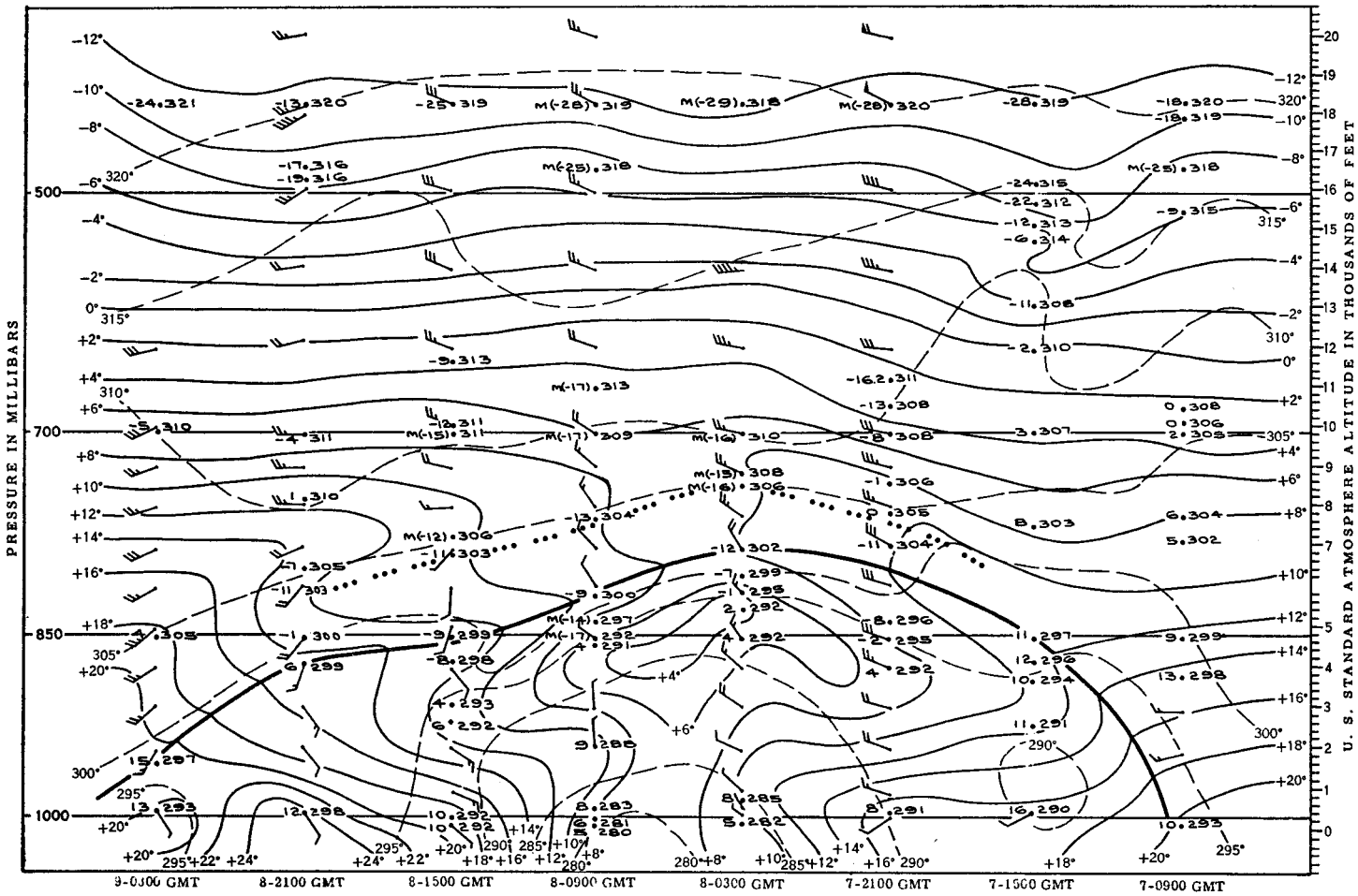

FIGURE 16.—Six-hourly time cross section over Mount Clemens, Mich. For clarity only the potential and dew point temperatures are plotted. The front is indicated by the heavy solid line, the subsidence inversion by the dotted line, the isotherms in ° C. by the light solid lines, and the potential temperature isotherms in ° A. by the dashed lines.

thickness and 1000-mb. height. The sea level weather chart for 1830 GMT, June 8 is illustrated in figure 7. Table 1 gives some relationships of thickness change to sea level pressure change and 500-mb. height change. The data are taken from figures 2, 5, and 6 which were obtained by graphical subtraction of succeeding carefully analyzed 1000-500-mb. thickness and 1000-mb height charts. For some of the raob stations included in the table, the listed 500-mb. height changes do not agree exactly with the results obtained by simply subtracting the height values as reported by these raob stations. This is because it is not possible to draw exactly for all the 500-mb. data as reported; some small corrections must be made. These corrections are slight and no discrepancies of any consequence have resulted.

The areas where warming in the 1000-500-mb. layer has actually been realized are the positive areas of 12-hour thickness change, as shown in figures 2, 5, and 6. At 0300 GMT, June 8 (fig. 2) the highest closed relative isallohypse shows a thickness of +200 feet, corresponding to an increase in mean virtual temperature of 3° C. for the entire 1000-500-mb layer. The main area of thickness increase is to the east-northeast of the main area of 1000-mb. height fall (surface pressure fall). The center of the Low at this time was following a track almost parallel to the line from 1000-mb. height falls to 1000-500-mb. thickness increase. Twelve hours later (fig. 5) the center of thickness change has almost doubled to a closed +400-foot relative isallohypse, indicating pronounced warm air advection, while the center of 1000-mb. height falls has deepened only about one third. The two change centers are still located relative to each other as in figure 2, except that now they are about twice as far apart. At this time the surface Low was moving at a speed of about 40 knots. By 0300 GMT, June 9 (fig. 6) the pronounced warm air advection shown in figure 5 has been greatly reduced and the center of thickness increase is now located almost directly south of the center of 1000-mb. height fall, which has maintained a closed —400-foot isallohypse. While the sea level Low continued to exhibit about the same central pressure, after 0300 GMT, June 9, it slowed down to 25–30 knots. Its direction of movement veered to almost directly east.

From the thermal wind equation [3] it is seen that veering wind with height indicates warm air advection, and backing wind with height indicates cold air advection.

Figures 8–13 are hodographs corresponding to the times of figures 1, 3, and 4. Since the thermal wind is parallel to the isotherms of mean virtual temperature, with warm air to the right, the component of the wind *at either bounding level* normal to the shear vector is a measure of the indicated advection. Or the indicated advection is proportional to the areas of the triangles composed of the winds at the two bounding levels and the thermal wind (or shear). The hodographs all indicate pronounced warm air advection.

At Mount Clemens, Mich., the amount of warming from 1500 GMT, June 7, when the station was in the cold air at the surface, to 0300 GMT, June 9, just after a surface warm front had passed, is shown by the upper air soundings in figure 14. Certainly, strong warm air advection has taken place at this station. The superadiabatic lapse rate between 850 and 800 mb. at 0300 GMT, June 9, is interesting both from warm air advection considerations and the occurrence of numerous tornadoes in the area beginning about 2330 GMT, June 8. While no detailed study of the various factors contributing to the cause of these disastrous storms was made for this paper, it is the opinion of the writers and other members of the WBAN Analysis Center staff that strong warm air advection in the lower levels did play a part in the genesis of these tornadoes.

The upper air soundings over Green Bay, Wis., at 0300 GMT and 1500 GMT, June 8 (fig. 15) also show warming in the lower levels. At 0300 GMT Green Bay was well into the cold air; at 1500 GMT a surface occlusion was located just west of the station. The hodograph for Green Bay at 0300 GMT, June 8 is shown in figure 9.

A 6-hourly time cross section over Rome, N. Y., is shown in figure 16. At the beginning of the cross section, 0900 GMT, June 7, a cold front was approaching Rome, followed by a cold dome, and at the end of the cross section a warm front was approaching the station. Below the front the cold core was over Rome at about 0600 GMT, June 8. Above the front, generally, warm air advection was occurring from 1500 GMT, June 7 to 0900 GMT, June 8. The lowest 1000-500-mb. thickness value occurred about 0600 GMT, June 8. From the figure it is apparent that the main advection below 500 mb. took place below about 750 mb. The 1000-mb. height continued to rise, even after the cold core had passed, until it reached a maximum value of 610 feet (sea level pressure, 1022 mb.) at 1500 GMT, June 8. It appears that this continued rise after 0600 GMT, June 8 must have been due to a density increase above the 500-mb. layer.

Several of the soundings exhibited double inversions. The lower one was caused by the front and the upper one was rather dry, and was taken to be a subsidence layer formed by the sinking motion of the cold dome. This inversion appears very abruptly between 1500 GMT and 2100 GMT, June 7. The cold front was rather active, producing numerous showers along both sides of the surface front. As soon as this active weather zone had passed, the subsidence inversion appeared.

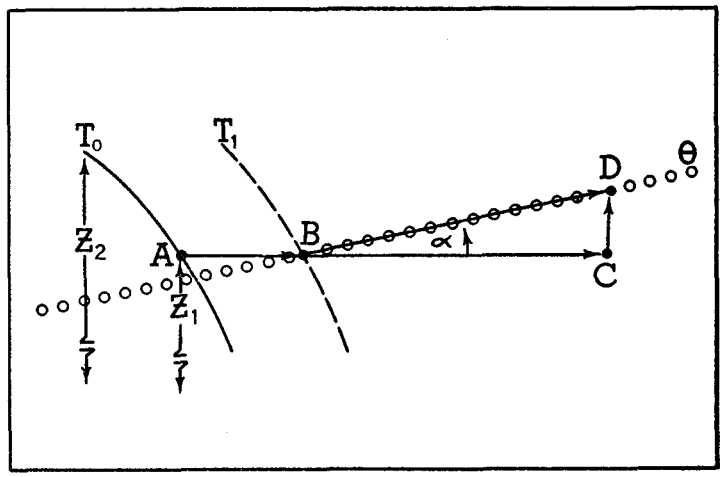

FIGURE 17.—Diagram illustrating the method used in computing vertical velocities. (See text.) T_0 and T_1 are thickness profiles at times T_0 and T_1 respectively. Z_1 and Z_2 are thickness values. The open-dotted line, θ, is an isentropic surface.

SOME SIMPLE COMPUTATIONS OF VERTICAL VELOCITIES

As stated previously, the regions of indicated warm air advection are those where the flow within a thickness layer is from higher to lower thickness values and therefore has a component against the thickness lines. However, it is seldom that the thickness lines move with the speed of the component normal to them. Rather, the thickness lines are considered to move with the speed of the front behind which they lie, 60 to 80 percent of the normal component for warm fronts and 70 to 90 percent for cold fronts [5]. That part of the normal component in excess of the displacement of the particular thickness lines, since it is directed toward denser air, represents flow upward along an isentropic surface until condensation is reached. If the component of the normal wind not used in the displacement of the thickness line, and the slope of a representative isentropic surface (that of the front) parallel to the normal component are known, the vertical velocity may be computed [5]. The foregoing principle is illustrated in figure 17, in which $\overline{AC}$ is the component of the mean wind or, in the case of linear change of wind with height, the component of the wind at either the upper or lower bounding surface of the thickness, taken normal to the thickness line; $\overline{AB}$ is the portion of $\overline{AC}$ that is used in the displacement of the thickness Z_1 from A to B; the thickness profile (greatly exaggerated) moves from T_0 to T_1; $\overline{BC}$ is the portion of $\overline{AC}$ that moves along the isentrope, θ; α is the angle made by the isentropic surface and the horizontal; and $\overline{CD}$ is the vertical velocity. From the figure $\overline{CD}=\overline{BC}\tan\alpha$.

Figure 1 was used in the computations of the components normal to the thickness lines. By comparing these displacements with the thickness chart 12 hours later (fig.

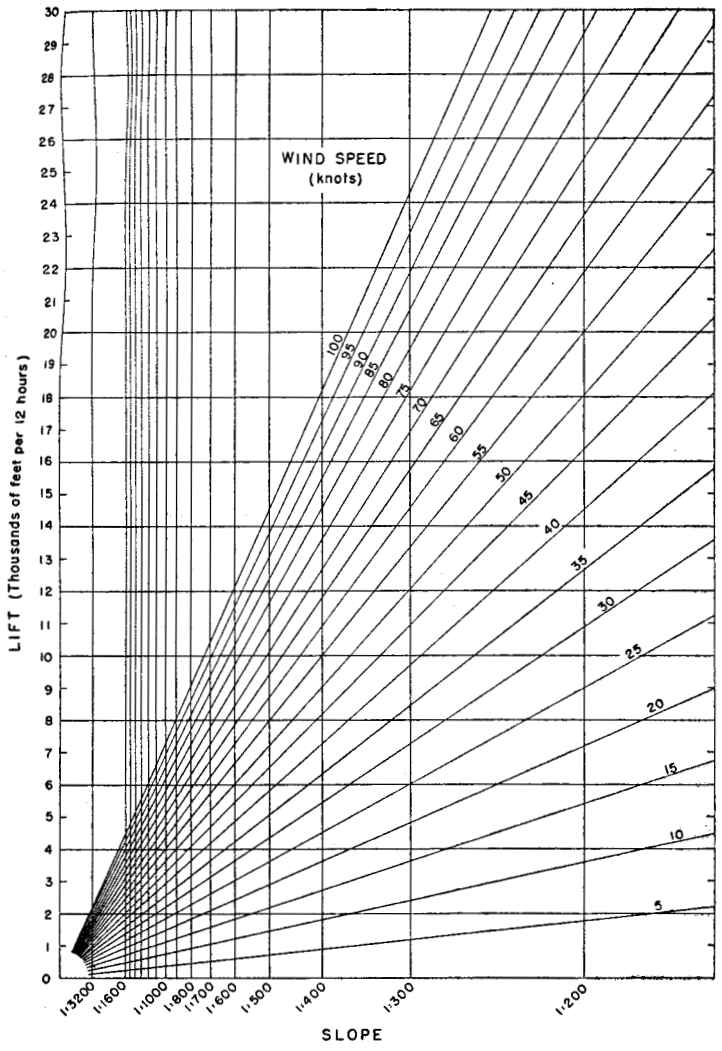

FIGURE 18.—Graph of the amount of lift in thousands of feet per 12 hours (ordinate), given the slope of the isentropic surface (abscissa) and the component of the normal wind (in knots) that is not accounted for by the movement of thickness lines. If the isentropic surface slope is negative, a particle will undergo subsidence.

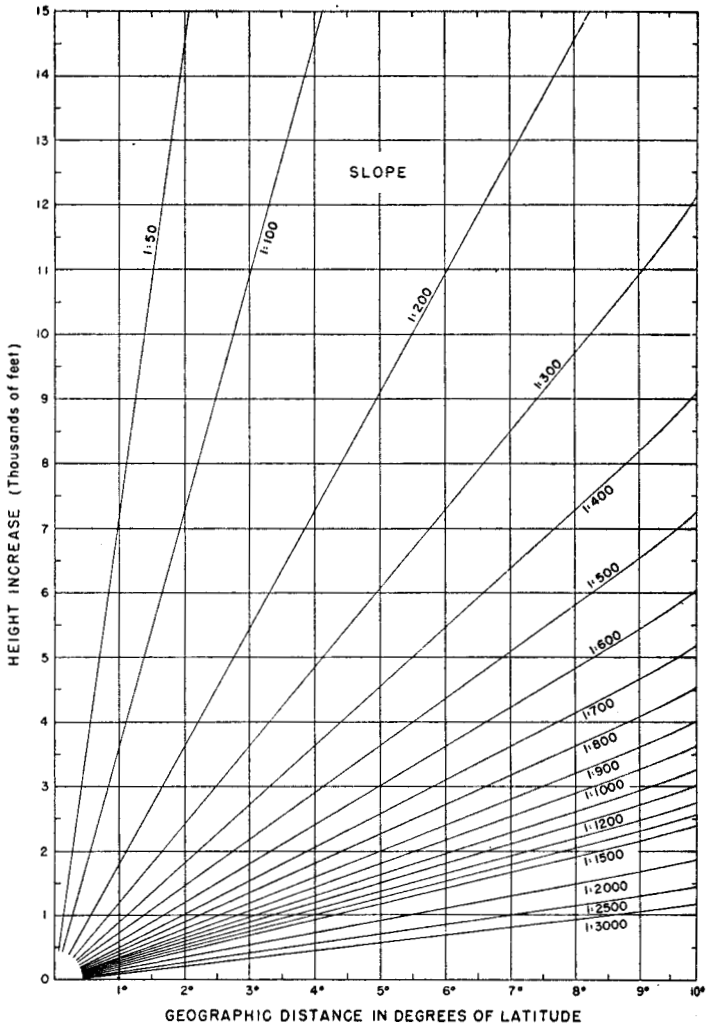

FIGURE 19.—Graph giving the slope of an isentropic surface, given the distance in degrees of latitude between two points (abscissa) and the difference in height in feet of the isentropic surface between these two points (ordinate). If the height of the isentropic surface decreases along the positive direction between two points, then the slope is negative.

3), the normal components that are not accounted for by the observed movements are obtained. Each "left over" component is then multiplied by the slope of the isentropic surface normal to the thickness line, and yields the vertical velocity. Figure 18 gives the amount of 12-hour lift in feet from the known values of isentropic slope (see fig. 19) and component normal to thickness lines that is not accounted for by displacement of the thickness lines. The 299° A. isentropic chart for 0300 GMT, June 8 is shown in figure 20, which also shows the advection arrows obtained from mean flow against 1000-500-mb. thickness lines.

The correlation between precipitation and vertical motion from 0300 GMT to 1500 GMT, June 8 is illustrated in figure 21. Figure 22 is a 299° A. isentropic chart for 1500 GMT, June 8. It is interesting to note that wherever warm air advection (thin arrows) is occurring the mean flow arrows are moving upslope along the isentropic surface, and where cold air advection (heavy arrows) is taking place the arrows are moving downslope. The correlation between precipitation and vertical motion from 1500 GMT, June 8 to 0300 GMT, June 9 is illustrated in figure 23.

At 1500 GMT, June 8 (fig. 3) rather pronounced warm air advection was indicated around the eastern periphery of the Low center. But 12 hours later (fig. 4) the cold front had swept into this area moving the thickness lines to the south. Therefore, the components of the wind normal to the thickness lines at 1500 GMT, June 8, that cannot be accounted for by advection of the thickness lines to their positions 12 hours later, are the normal components plus the speed of the southerly movement of the lines. This results in strong components, which yield rather high vertical velocities around the eastern edge of the Low center (fig. 23). Such values are in agreement with the well-founded theory of horizontal convergence around Low centers.

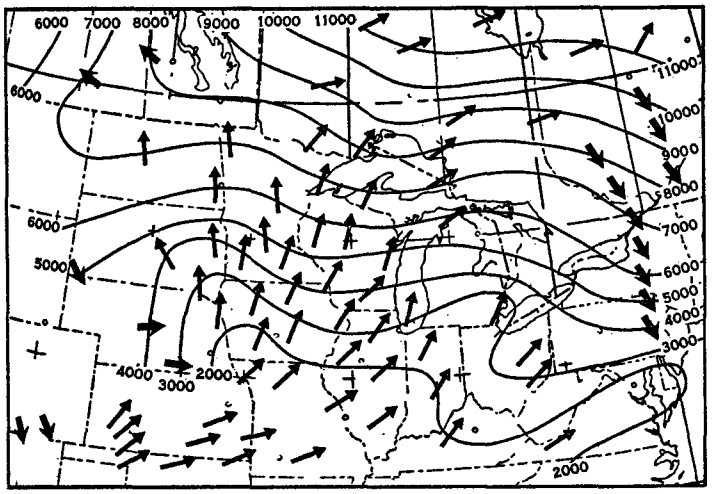

FIGURE 20.—229° A. isentropic chart for 0300 GMT, June 8, 1953. Warm and cold air advection, from considerations of mean flow against thickness lines, is indicated by the thin and heavy arrows, respectively.

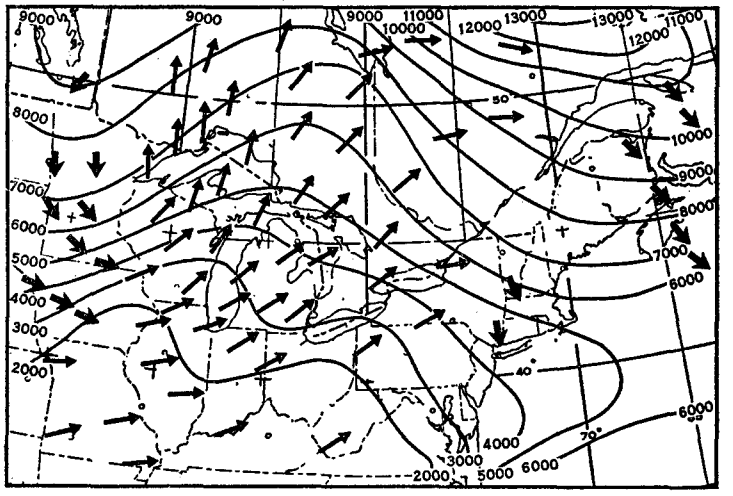

FIGURE 22.—229° A. isentropic chart for 1500 GMT, June 8, 1953.

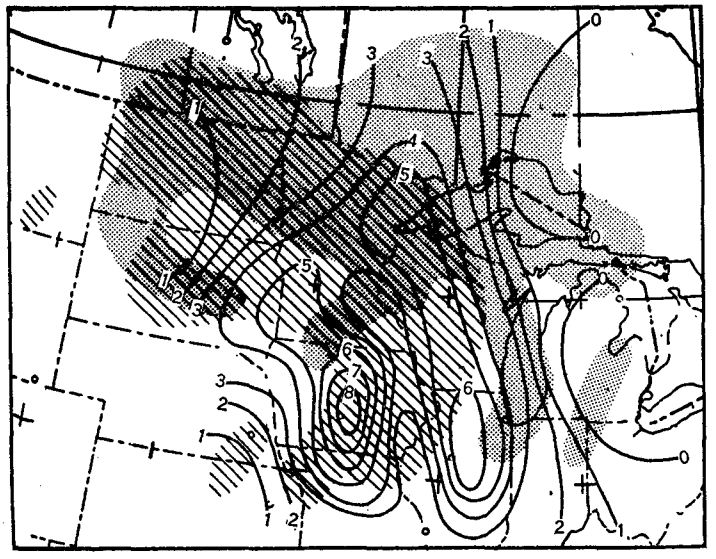

FIGURE 21.—Computed 12-hour lift in thousands of feet from 0300 GMT to 1500 GMT, June 8, 1953. The area where precipitation has occurred from 0330 GMT through 0930 GMT, June 8, is crosshatched, that from 1230 GMT through 1530 GMT, June 8, is shaded.

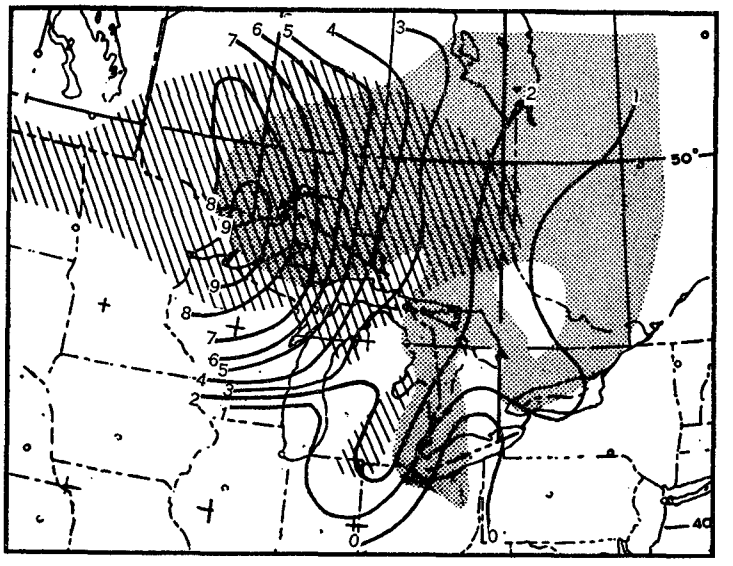

FIGURE 23.—Computed 12-hour lift from 1500 GMT, June 8, to 0300 GMT, June 9, 1953. The area where precipitation has occurred from 1530 GMT through 2130 GMT, June 8, is crosshatched, that from 0030 GMT, June 9, through 0330, GMT, June 9, is shaded.

CONCLUDING REMARKS

The main idea in this study of warm air advection has been to present a clear picture of the relationship between 1000-500-mb. thickness changes and sea level pressure changes. The method of computing vertical velocities, admittedly, is rough and extremely subjective, but it has the advantage of furnishing comparatively quick results.[1] Although the correlation between vertical motion and precipitation areas is favorable in this case, the notion needs considerable refinement. While this study has dealt primarily with warm air advection, many of the ideas employed are equally applicable to cold air advection.

[1] Some notable and more refined methods of computing vertical velocities have been developed by research units of the United States Air Force at New York University and by members of the New York University staff and the United States Weather Bureau. (For instance, see [6].)

REFERENCES

1. J. M. Austin, "Cloudiness and Precipitation in Relation to Frontal Lifting and Horizontal Convergence," 46 pp. (See pp. 15–16.) *Papers in Physical Oceanography and Meteorology*, vol. IX, No. 3, Massachusetts Institute of Technology and Woods Hole Oceanographic Institution, Cambridge and Woods Hole, Mass., 1943.
2. G. A. Lott, "An Extraordinary Rainfall Centered at Hallett, Okla.," *Monthly Weather Review*, vol. 81, No. 1, Jan. 1953, pp. 1–10.
3. H. R. Byers, *General Meteorology*, McGraw-Hill Book Co., Inc., New York, 1944, pp. 367–380, 211–214.
4. R. C. Bungaard, "A Procedure of Short-Range Weather Forecasting," *Compendium of Meteorology*, American Meteorological Society, Boston, 1952, pp. 766–795.

5. S. Petterssen, *Weather Analysis and Forecasting*, McGraw-Hill Book Co., Inc., New York, 1940, pp. 407–411.

6. J. E. Miller, et al, *A Study of Vertical Motion in the Atmosphere*, Dept. of Meteorology, New York University, N. Y., Feb. 1946, 68 pp.

CORRECTION

MONTHLY WEATHER REVIEW, vol. 81, No. 2, February 1953, page 37: Sentence beginning in line 1 should read "They indicate that wind waves and swell do have the characteristics of the surface waves."

Page 35, figure 3: Isopleth at center over intersection of cross lines should be labeled "8" instead of "9."

U. S. GOVERNMENT PRINTING OFFICE: 1953